Vol 464|29 April 2010|doi:10.1038/nature08953

LETTERS

Dipolar collisions of polar molecules in the quantum regime

K.-K. Ni[1]*, S. Ospelkaus[1]†*, D. Wang[1], G. Quéméner[1], B. Neyenhuis[1], M. H. G. de Miranda[1], J. L. Bohn[1], J. Ye[1] & D. S. Jin[1]

Ultracold polar molecules offer the possibility of exploring quantum gases with interparticle interactions that are strong, long-range and spatially anisotropic. This is in stark contrast to the much studied dilute gases of ultracold atoms, which have isotropic and extremely short-range (or 'contact') interactions. Furthermore, the large electric dipole moment of polar molecules can be tuned using an external electric field; this has a range of applications such as the control of ultracold chemical reactions[1], the design of a platform for quantum information processing[2–4] and the realization of novel quantum many-body systems[5–8]. Despite intense experimental efforts aimed at observing the influence of dipoles on ultracold molecules[9], only recently have sufficiently high densities been achieved[10]. Here we report the experimental observation of dipolar collisions in an ultracold molecular gas prepared close to quantum degeneracy. For modest values of an applied electric field, we observe a pronounced increase in the loss rate of fermionic potassium–rubidium molecules due to ultracold chemical reactions. We find that the loss rate has a steep power-law dependence on the induced electric dipole moment, and we show that this dependence can be understood in a relatively simple model based on quantum threshold laws for the scattering of fermionic polar molecules. In addition, we directly observe the spatial anisotropy of the dipolar interaction through measurements of the thermodynamics of the dipolar gas. These results demonstrate how the long-range dipolar interaction can be used for electric-field control of chemical reaction rates in an ultracold gas of polar molecules. Furthermore, the large loss rates in an applied electric field suggest that creating a long-lived ensemble of ultracold polar molecules may require confinement in a two-dimensional trap geometry to suppress the influence of the attractive, 'head-to-tail', dipolar interactions[11–14].

Dipolar interactions have been explored in several atom-gas experiments using the magnetic dipole moments of atoms[15,16]; however, this interaction is intrinsically orders of magnitude weaker than the dipolar interaction between typical polar molecules. Ultracold gases of polar molecules thus allow the possibility of realizing strong and, therefore, relatively long-range interactions. For example, polar molecules confined in optical lattice potentials could be used to create a system in which the interactions between particles at neighbouring sites is as strong as the on-site interactions now commonly realized with atoms. This longer-range interaction for polar molecules will allow access to a new regime of strongly correlated quantum gases with quantum phase transitions, such as to supersolid phases for bosons[17–19] and to topological superfluid phases for fermions[20]. Another important difference between magnetic and electric dipolar interactions is that the strength of the effective electric dipole moment can be tuned using an applied electric field. In addition to its obvious utility in controlling the interaction strength in dipolar quantum gases, the electric-field dependence could be exploited in the development of new quantum computing schemes or in the control of ultracold chemical reactions.

We perform our experiments with an ultracold gas of $^{40}K^{87}Rb$ molecules prepared in a single nuclear hyperfine state within the rovibronic (rotational–vibrational–electronic) ground state, $^1\Sigma^+$ (refs 10, 21). The gas is confined in a pancake-shaped optical dipole trap, which is formed by overlapping two horizontally propagating, elliptically shaped laser beams with wavelengths of $\lambda = 1{,}064$ nm. Typical harmonic trapping frequencies are $\omega_x = 2\pi \times 40$ Hz and $\omega_z = 2\pi \times 280$ Hz in the horizontal and vertical directions, respectively. The $^{40}K^{87}Rb$ molecules have a permanent electric dipole moment of 0.57 Debye (D)[10], where $1\,\mathrm{D} = 3.336 \times 10^{-30}$ C m. However, the effective molecular dipole moment in the laboratory frame is zero in the absence of an external electric field. When an external electric field is applied, the molecules begin to align with the field and have an induced dipole moment, d, that increases as shown in the inset of Fig. 1b. This figure covers the range of applied electric field that we currently access experimentally, which corresponds to an accessible dipole moment range of 0–0.22 D. In our set-up, the external electric field points up (in the z direction), parallel to the tight axis of the optical trap. Thus, the spatially anisotropic dipolar interactions will be predominantly repulsive for molecules colliding in the horizontal direction (side by side) and predominantly attractive for molecules approaching each other along the vertical direction (head to tail).

In an ultracold gas, the quantum statistics of the particles has an essential role in the interactions. Our $^{40}K^{87}Rb$ molecules are fermions prepared in a single internal quantum state at a temperature equal to 1.4 times the Fermi temperature. Therefore, the quantum statistics requires that the wave function for two colliding molecules be antisymmetric with respect to molecule exchange. Considering the relative angular momentum of two colliding molecules, this means that scattering can only proceed via partial waves with odd l, the angular momentum quantum number, and will be dominated by p-wave scattering ($l = 1$) at ultralow temperature. Previous work at zero electric field (without long-range dipolar interactions) showed that the lifetime of the trapped $^{40}K^{87}Rb$ molecules is limited by atom-exchange chemical reactions that proceed by means of p-wave scattering[22]. In our experiments, the typical translational temperature of the molecular gas is 300 nK and the energy height of the p-wave barrier for $^{40}K^{87}Rb$ molecules corresponds to a temperature of approximately 24 μK (ref. 30). As the barrier height is much larger than the typical collision energies, scattering rates in the molecular

[1]JILA, NIST and University of Colorado, Department of Physics, University of Colorado, Boulder, Colorado 80309-0440, USA. †Present address: Max Planck Institute for Quantum Optics, D-85748 Garching, Germany.
*These authors contributed equally to this work.

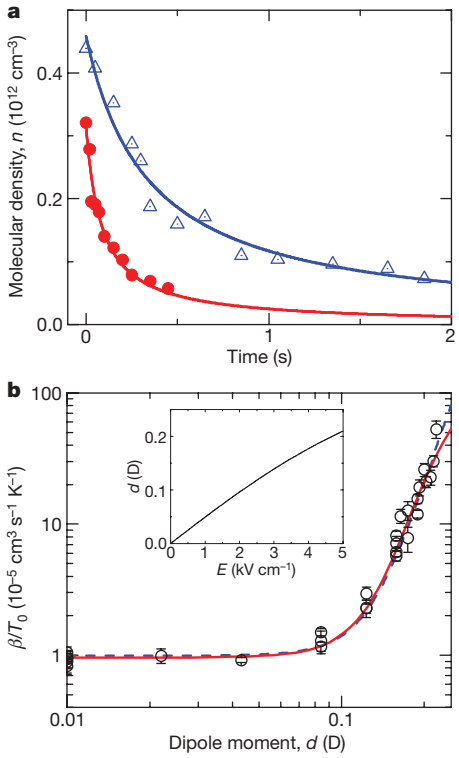

Figure 1 | Two-body inelastic loss for fermionic polar molecules. a, We extract the inelastic loss rate coefficient, β, from a fit (solid lines) to the measured time evolution of the trapped molecular gas density. Data are shown here for induced dipole moments of $d = 0.08$ D (open triangles) and $d = 0.19$ D (filled circles), and $T_0 = 300$ nK. **b**, Data points show β/T_0 plotted as a function of d. The dashed line shows a fit to a simple model based on the quantum threshold behaviour for tunnelling through a dipolar-interaction-modified p-wave barrier (see text). The solid line shows the result of a more complete quantum scattering calculation. Inset, the calculated dependence of d on the applied electric field, E. Error bars, 1 s.d.

cloud are determined by the tunnelling rate through the centrifugal barrier and the molecule-gas lifetime is relatively long (on the order of 1 s)[22].

In this Letter, we investigate the effect of electric dipolar interactions on collisions and find an unexpectedly large effect even for our relatively modest range of applied electric fields. We measure the molecular loss rate by monitoring the time evolution of the average number density of trapped molecules, n (Fig. 1a). We fit the data to the solution of

$$\frac{dn}{dt} = -\beta n^2 - \alpha n \qquad (1)$$

shown as solid lines in Fig. 1a.

The first term on the right-hand side of equation (1) accounts for number loss, and we extract the measured two-molecule inelastic loss rate coefficient, β (which is twice the collisional event rate), from the fit. The second term describes the density decrease arising from heating of the trapped gas during the measurement, which is such that $n \propto T^{-3/2}$. In a single measurement, we observe an increase in temperature that is at most 50%. In subsequent analysis, we fit a straight line to the measured temperature as a function of time and obtain the slope, c. In equation (1), we then use $\alpha = (3/2)c/(T_0 + ct)$, where T_0 is the initial temperature of the gas (see also ref. 22).

Figure 1b shows a summary of our experimental data in a plot of β/T_0 as a function of d. We plot the ratio β/T_0 because the Wigner threshold law for p-wave scattering predicts that β scales linearly with T, a temperature dependence that we previously verified at $d = 0$ D (ref. 22). For the data in Fig. 1, T_0 ranged from 250 nK to 500 nK. In Fig. 1b, we see that dipolar interactions have a pronounced effect on the inelastic collision rate. At low electric field, where $d < 0.1$ D, we observe no significant modification to the loss rate at zero electric field (which is plotted at $d = 0.01$ D for inclusion on the logarithmic scale). However, for higher electric fields, we observe a rapidly increasing loss rate, with an increase in β/T_0 of well over an order of magnitude by $d = 0.2$ D. Fitting the data for $d > 0.1$ D, we find that the inelastic loss rate coefficient has a power-law dependence on d: $\beta/T_0 \propto d^p$, where $p = 6.1 \pm 0.8$.

To understand this strong dependence of the inelastic loss rate on the electric field, we consider a relatively simple quantum threshold model in which the loss is assumed to be due to collisions between fermionic molecules that proceed by means of tunnelling through a p-wave centrifugal barrier followed by loss with unit probability at short range[14]. The fact that we do not observe any resonant oscillations as a function of electric field (Fig. 1b) is consistent with there being a very high loss probability for molecules reaching short range. In an applied electric field, the long-range dipole–dipole interaction, which is proportional to R^{-3}, R being the intermolecular separation, significantly modifies the height of the p-wave barrier and thus changes the inelastic collision rate. Moreover, the fact that the dipole–dipole interaction is spatially anisotropic means that the p-wave barrier height will be different for $m_l = 0$ and $m_l = \pm 1$ scattering, where the quantum number m_l describes the projection of the relative orbital angular momentum (quantum number l) onto the electric field direction. In particular, the attractive nature of dipole–dipole interactions for polar molecules colliding head to tail lowers the barrier for $m_l = 0$ collisions, whereas the repulsive dipole–dipole interaction for polar molecules colliding side by side raises the barrier for $m_l = \pm 1$ collisions. In Fig. 2a, b we show these effects schematically, and in Fig. 2c we show the calculated maximum heights of the respective $m_l = 0$ and $m_l = \pm 1$ collisional barriers, V_0 and V_1, as functions of d.

In our simple model, we assume that the collision rate follows the Wigner threshold law for p-wave inelastic collisions, that is, $\beta \propto T/V^{3/2}$ ($V = V_0$, V_1). For large values of d, V_0 is significantly smaller than V_1 and the loss will proceed predominantly through head-to-tail attractive collisions of the polar molecules. In this regime, V_0 scales as d^{-4} and the model predicts that β/T_0 will increase with a characteristic dependence on the sixth power of d for $d > 0.1$ D (ref. 14). This prediction is in excellent agreement with our measured dependence of the loss rate on d for $d > 0.1$ D (Fig. 1b).

For a quantitative description of the inelastic collisional rate over our full range of experimentally accessible dipole moments, we include contributions from both $m_l = 0$ and $m_l = \pm 1$ collisions, and we calculate the barrier heights using adiabatic potential curves that include mixing with higher-l partial waves (Fig. 2c). We fit the prediction of this quantum threshold model to our data using two fit parameters: a scaling factor, γ, that can be interpreted as the loss probability when the collision energy equals the height of the barrier; and a factor, b, that multiplies the coefficient of the van der Waals interaction, C_6. The resulting theoretical prediction (Fig. 1b, dashed line) agrees very well with our experimental data (Fig. 1b, open circles); the fit yields $\gamma = 0.35 \pm 0.08$ and $b = 2.4 \pm 0.9$. For comparison with the simple quantum threshold model, Fig. 1b also shows (solid line) the result of a more complete quantum scattering calculation. This calculation employs a strong absorptive potential at short range but captures the long-range physics and uses C_6 as the single fit parameter. This fit also agrees well with the experimental data, and gives $C_6 = 21{,}000 \pm 7{,}000$ a.u. (1 a.u. $= E_h a_0^6$, where $E_h = 4.36 \times 10^{-18}$ J and $a_0 = 0.529$ Å), which is consistent with the predicted value of $C_6 = 16{,}130$ a.u. (ref. 30).

Accompanying the increased inelastic loss rates for increasing d, we observe an increased heating rate for the polar-molecule gas. In Fig. 3, we plot the fractional heating rate, $\dot{T}/T_0$, normalized by the initial n and T_0, as a function of d. The heating rate $\dot{T} = c$ is extracted using a linear fit to the temperature of the molecular cloud measured as a function of time over a period sufficiently long to allow T to

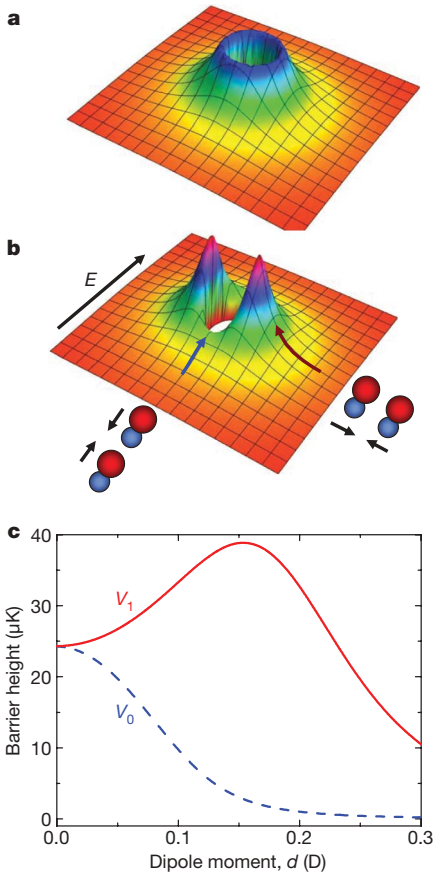

Figure 2 | A *p*-wave centrifugal barrier for dipolar collisions between fermionic polar molecules. **a**, The effective intermolecular potential for fermionic molecules at zero electric field. At intermediate intermolecular separation, two colliding molecules are repelled by a large centrifugal barrier for *p*-wave collisions. **b**, For a relatively small applied electric field, the spatially anisotropic dipolar interactions reduce the barrier for head-to-tail collisions and increase the barrier for side-by-side collisions. **c**, Height of the *p*-wave barrier as a function of dipole moment. Dipolar interactions lower the centrifugal barrier for $m_l = 0$ collisions (V_0) and raise the barrier for $m_l = \pm 1$ collisions (V_1). The lowering of the $m_l = \pm 1$ barrier at very large dipole moments is due to mixing with higher-l partial waves ($l = 3, 5, 7, \ldots$).

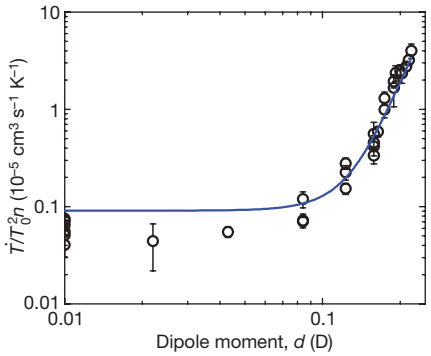

Figure 3 | Normalized fractional heating rate, $\dot{T}/T_0^2 n$, as a function of dipole moment. The heating rate is extracted using a linear fit to the initial temperature increase and is then normalized by the initial density and temperature of the ensemble. The solid line is the expected heating rate, given by $\dot{T}/T_0^2 n = (\beta/T_0)/12$ (see text). Typical initial conditions for these data are $n = 0.3 \times 10^{12}$ cm^{-3} and $T_0 = 0.5$ μK, and the absolute heating rate ranges from 0.1 μK s^{-1} at zero electric field to 2 μK s^{-1} at our highest electric fields. Error bars, 1 s.d.

increase by approximately 20–30%. We have developed a simple thermodynamic model for heating that is directly caused by the inelastic loss. We consider the energy lost from the gas when molecules are removed in inelastic collisions, and assume that the gas stays in thermal equilibrium. In this model (Supplementary Information), the heating arises solely from density-dependent loss of particles from the trap[23], where the particles removed by inelastic collisions have, on average, lower energies than typical particles in the gas. One way to understand this heating mechanism is to note that inelastic collisions preferentially remove particles from the centre of the trap, where the number density is the highest and the particles have the lowest potential energy from the trap. We also include in our calculations a competing, 'cooling', effect that comes from the fact that the *p*-wave inelastic collision rate increases linearly with the collision energy. Including these two competing effects, we obtain $\dot{T}/T_0^2 n = (\beta/T_0)/12$ (Supplementary Information). Remarkably, this simple prediction (Fig. 3, solid line), made using the β/T_0 values from the fit to our loss rate data in Fig. 1 with no additional free parameter, agrees very well with the independently measured heating rates of the molecular gas.

The anisotropy of the dipole–dipole interaction is shown directly in an anisotropic distribution of molecules in the trap. The average energy per particle, which we measure from the expansion of the gas following a sudden release from the trap, can be different in the vertical and horizontal directions. In the following, we present measurements of the time evolution of the expansion energy in these two directions for different values of d. To probe the spatial anisotropy of dipolar collisions, we start by adding energy along one direction of the cylindrically symmetric trap using parametric heating. Here we modulate the power of both optical trapping beams at twice the relevant harmonic trapping frequency, for 50 ms (z direction) or 100 ms (x and y directions). We then wait 100 ms before quickly increasing the electric field (in less than 1 μs) to the desired final value and measuring the time dependence of the vertical and horizontal 'temperatures' of the cloud, respectively denoted T_z and T_x. These quantities simply correspond to the measured expansion energies in the two directions. We note that this type of measurement is commonly used in experiments on ultracold atom gases to measure the elastic collision cross-section[24].

Figure 4 shows the experimental data from these rethermalization experiments for three values of d and under two initial conditions: $T_z > T_x$ (Fig. 4a–c) and $T_z < T_x$ (Fig. 4d–f). For $d = 0$ D (Fig. 4a, d), T_z and T_x equilibrate very slowly, on a timescale of approximately 4 s. Because $d = 0$ D, there are no dipolar interactions and the data agree with our expectation of very slow equilibration for spin-polarized fermions. Indeed, this is the longest rethermalization time we observed in our trap, and therefore the data are consistent with there being no elastic collisions and only technical imperfections such as a small cross-dimensional coupling in the trapping potential.

In an applied electric field, the elastic collision cross-section due to long-range dipolar interactions is predicted to increase in proportion to d^4 (ref. 25). For the case in which initially $T_z > T_x$ (Fig. 4b, c), our data show that T_z and T_x approach each other in what seems on casual inspection to be cross-dimensional rethermalization. The timescale for this apparent rethermalization even decreases steeply as d increases, as might be expected. However, we note that in Fig. 4c the temperatures cross each other, which is inconsistent with rethermalization driven by elastic collisions. Even more striking is the fact that the thermodynamic behaviour of the gas is completely different when the gas initially has $T_z < T_x$. In this case, T_z and T_x do not equilibrate during the measurement time (Fig. 4e, f).

The explanation for these surprising observations comes from the spatially anisotropic nature of inelastic dipole–dipole collisions and the fact that the molecular gas undergoes number loss. We have seen (Fig. 3) that loss due to inelastic collisions heats the gas, and we can quantitatively understand this heating rate by considering the effect of molecule loss on the average energy per particle. We can adapt the model of heating and inelastic collisions described above to allow the average energy per particle, or 'temperature', to be different in the

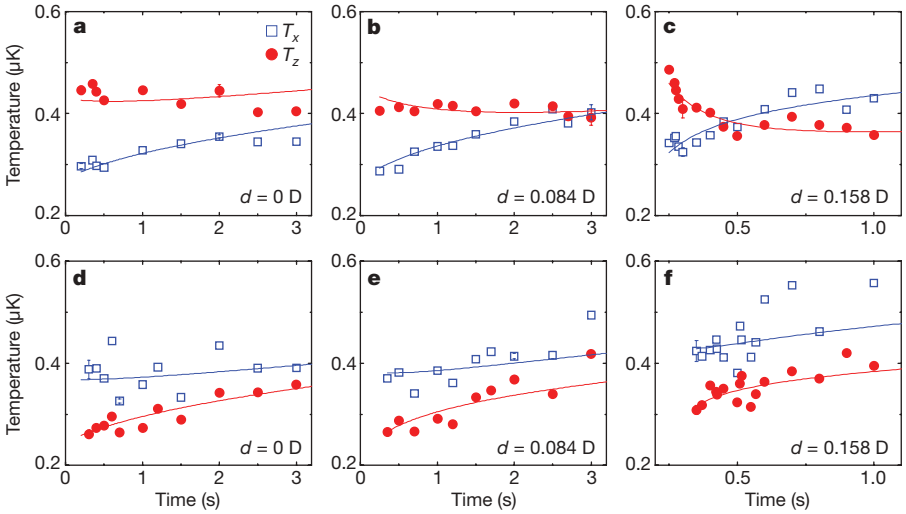

Figure 4 | Apparent cross-dimensional rethermalization in the polar molecule gas. Shown as a function of dipole moment, d, for $T_z > T_x$ (**a**–**c**) and $T_z < T_x$ (**d**–**f**). The experimental data reveal a striking difference between heating the gas in the vertical direction (**a**–**c**) and heating it in the horizontal directions (**d**–**f**), and thus provide evidence for the strong anisotropic characteristic of dipolar interactions (see text). The electric field is applied along the z direction. Error bars show 1-s.d. uncertainties for a few example points.

two trap directions. The model then predicts that the dominant head-to-tail collisions ($m_l = 0$) will lead to heating in the x and y directions but cooling in the z direction. Side-by-side collisions ($m_l = \pm 1$), however, should contribute to heating in the z direction but produce no temperature change in the x and y directions (Methods and Supplementary Information). To compare this model with our rethermalization-type data, we fix the d-dependent β using the fit to our data in Fig. 1 (solid line). This fixes both the time evolution of the molecule number as well as the heating rates in the two trap directions. We then accommodate possible elastic collision effects in the model by adding a term that would exponentially drive the energy difference between the two directions to zero. Figure 4 shows a comparison between the results of the model (solid lines) and our experimental data. Although the model uses few free parameters (only the elastic collision cross-section in addition to the initial values of n, T_x and T_z), it provides excellent agreement with the experimental data.

Our observations provide clear evidence of the anisotropic nature of the dipole–dipole interactions through the observed anisotropy in the apparent rethermalization. From the agreement of the data with the model, we conclude that the rethermalization behaviour is actually dominated by the anisotropic nature of the inelastic collisions. This raises the question of what then can be concluded about the elastic collisions. The best-fit value for the elastic collision cross-section is finite and increases as d increases. This is consistent with the prediction that the elastic collision rate for polar molecules will scale as d^4 (ref. 25); furthermore, the best-fit values agree with the prediction of cross-sections on the order of $\sigma_{el} = 7 \times 10^{-8}\,\mathrm{cm^2\,s^{-1}\,D^{-4}}$ (ref. 25). However, the presence of inelastic loss and the resulting anisotropic heating make it difficult to accurately extract a measured value of the elastic cross-section for a more precise comparison with theory.

The results presented here demonstrate that modest applied electric fields can drastically alter the interactions of fermionic polar molecules in the quantum regime. In future efforts aimed at advancing the study of many-body phenomena in dipolar molecular quantum systems, it will be necessary to protect the gas from strong inelastic loss and heating[11,12,26]. This could be accomplished by finding a molecular system without two-body inelastic loss channels, but the demonstration here of strong spatial anisotropy in inelastic collisions of polar molecules suggests that, alternatively, studying a two-dimensional trapped gas will be a promising route to realizing a long-lived quantum gas of polar molecules with dipole–dipole interactions. This could be achieved with, for example, polar molecules confined in an array of pancake-shaped dipole traps in a one-dimensional optical lattice configuration[11,12]. Even when short-range inelastic loss processes are suppressed, the attractive part of the long-range dipole–dipole interaction could still give rise to correlations between neighbouring pancake-shaped dipole traps in the one-dimensional optical lattice[27,28].

METHODS SUMMARY

For the fit to a quantum threshold model[14] in Fig. 1b, we write the inelastic loss rate coefficient as $\beta = K_0 T_z + 2K_1 T_x$, the sum of two terms corresponding respectively to $m_l = 0$ and $m_l = \pm 1$ scattering, and we assume that $T_z = T_x = T$. The d-dependent coefficients, K_0 and K_1, are obtained using

$$K = \gamma \frac{3\pi\hbar^2}{\sqrt{2\mu^3 V^{3/2}}} k_B$$

where K and V respectively equal K_0 and V_0 or K_1 and V_1, μ is the reduced mass of the colliding molecules, $\hbar$ is Planck's constant divided by 2π and k_B is Boltzmann's constant. The barrier heights, V_0 and V_1, are taken to be the respective maximum energies of the long-range adiabatic potential, $V(R)$, evaluated in a basis set of partial waves, $|lm_l\rangle$ (ref. 14), for $m_l = 0$ and $m_l = \pm 1$. The potential $V(R)$ includes a repulsive centrifugal term, $\hbar^2 l(l+1)/(2\mu R^2)$, an attractive isotropic van der Waals interaction, $-bC_6/R^6$, and the dipolar interaction. We use only two fit parameters, b and γ, when fitting this model to the measurements of β/T_0 versus d.

The solid lines in Fig. 4 are a fit of the measured time evolution of n, T_z and T_x to the numerical solution of the following three differential equations (Supplementary Information):

$$\frac{dn}{dt} = -(K_0 T_z + 2K_1 T_x)n^2 - \frac{n}{2T_z}\frac{dT_z}{dt} - \frac{n}{T_x}\frac{dT_x}{dt}$$

$$\frac{dT_z}{dt} = \frac{n}{4}(-K_0 T_z + 2K_1 T_x)T_z - \frac{2\Gamma_{el}}{3}(T_z - T_x) + a_{bg} \quad (2)$$

$$\frac{dT_x}{dt} = \frac{n}{4}K_0 T_z T_x + \frac{\Gamma_{el}}{3}(T_z - T_x) + a_{bg} \quad (3)$$

Here we have allowed for a difference in the average energies per particle in the two trap directions, T_z and T_x, such that $\beta = K_0 T_z + 2K_1 T_x$. For the fits, we fix the d-dependent coefficients K_0 and K_1 using the previous fit to the inelastic loss rate data in Fig. 1. In addition to heating due to inelastic loss, we include a measured background heating rate of $a_{bg} = 0.01\,\mu\mathrm{K\,s^{-1}}$. The elastic collision rate in equations (2) and (3) is given by $\Gamma_{el} = n\sigma_{el}v/N_{coll}$, where the elastic collision cross-section, σ_{el}, is a fit parameter, $v = \sqrt{8k_B(T_z + 2T_x)/3\pi\mu}$ and the constant N_{coll} can be thought of as the mean number of collisions per particle required for rethermalization. We use $N_{coll} = 4.1$, which was computed for p-wave collisions[29]; however, we note that N_{coll} depends on the angular dependence of the scattering and may be different for dipolar elastic collisions.

Received 15 January; accepted 23 February 2010.

1. Krems, R. V. Cold controlled chemistry. *Phys. Chem. Chem. Phys.* **10,** 4079–4092 (2008).
2. DeMille, D. Quantum computation with trapped polar molecules. *Phys. Rev. Lett.* **88,** 067901 (2002).
3. Andre, A. *et al.* A coherent all-electrical interface between polar molecules and mesoscopic superconducting resonators. *Nature Phys.* **2,** 636–642 (2006).
4. Yelin, S. F., Kirby, K. & Côte, R. Schemes for robust quantum computation with polar molecules. *Phys. Rev. A* **74,** 050301 (2006).
5. Micheli, A., Brennen, G. K. & Zoller, P. A toolbox for lattice-spin models with polar molecules. *Nature Phys.* **2,** 341–347 (2006).
6. Lahaye, T., Menotti, C., Santos, L., Lewenstein, M. & Pfau, T. The physics of dipolar bosonic quantum gases. *Rep. Prog. Phys.* **72,** 126401 (2009).
7. Pupillo, G., Micheli, A., Büchler, H. P. & Zoller, P. in *Cold Molecules: Theory, Experiment, Applications* (eds Krems, R. V., Stwalley, W. C. & Friedrich, B.) 421–469 (CRC, 2009).
8. Baranov, M. Theoretical progress in many-body physics with ultracold dipolar gases. *Phys. Rep.* **464,** 71–111 (2008).
9. Carr, L. D., DeMille, D., Krems, R. V., &. Ye. J. Cold and ultracold molecules: science, technology and applications. *N. J. Phys.* **11,** 055049 (2009).
10. Ni, K.-K. *et al.* A high-phase-space-density gas of polar molecules. *Science* **322,** 231–235 (2008).
11. Micheli, A. *et al.* Cold polar molecules in two-dimensional traps: tailoring interactions with external fields for novel quantum phases. *Phys. Rev. A* **76,** 043604 (2007).
12. Büchler, H. P. *et al.* Strongly correlated 2D quantum phases with cold polar molecules: controlling the shape of the interaction potential. *Phys. Rev. Lett.* **98,** 060404 (2007).
13. Li, Z. & Krems, R. V. Inelastic collisions in an ultracold quasi-two-dimensional gas. *Phys. Rev. A* **79,** 050701 (2009).
14. Quéméner, G. & Bohn, J. L. Strong dependence of ultracold chemical rates on electric dipole moments. *Phys. Rev. A* **81,** 022702 (2010).
15. Stuhler, J. *et al.* Observation of dipole-dipole interaction in a degenerate quantum gas. *Phys. Rev. Lett.* **95,** 150406 (2005).
16. Vengalattore, M. *et al.* Spontaneously modulated spin textures in a dipolar spinor Bose-Einstein condensate. *Phys. Rev. Lett.* **100,** 170403 (2008).
17. Gral, K., Santos, L. & Lewenstein, M. Quantum phases of dipolar bosons in optical lattices. *Phys. Rev. Lett.* **88,** 170406 (2002).
18. Capogrosso-Sansone, B., Trefzger, C., Lewenstein, M., Zoller, P. & Pupillo, G. Quantum phases of cold polar molecules in 2D optical lattices. *Phys. Rev. Lett.* (in the press); preprint at ⟨http://arxiv.org/abs/0906.2009⟩ (2009).
19. Pollet, L., Picon, J. D., Büchler, H. P. & Troyer, M. Supersolid phase with cold polar molecules on a triangular lattice. Preprint at ⟨http://arxiv.org/abs/0906.2126⟩ (2009).
20. Cooper, N. R. & Shlyapnikov, G. V. Stable topological superfluid phase of ultracold polar fermionic molecules. *Phys. Rev. Lett.* **103,** 155302 (2009).
21. Ospelkaus, S. *et al.* Controlling the hyperfine state of rovibronic ground state polar molecules. *Phys. Rev. Lett.* **104,** 030402 (2010).
22. Ospelkaus, S. *et al.* Quantum-state controlled chemical reactions of ultracold potassium-rubidium molecules. *Science* **327,** 853–857 (2010).
23. Masuhara, N. *et al.* Evaporative cooling of spin-polarized atomic hydrogen. *Phys. Rev. Lett.* **61,** 935–938 (1988).
24. Monroe, C. R., Cornell, E. A., Sackett, C. A., Myatt, C. J. & Wieman, C. E. Measurement of Cs-Cs elastic scattering at $T=30\ \mu K$. *Phys. Rev. Lett.* **70,** 414–417 (1993).
25. Bohn, J. L., Cavagnero, M. & Ticknor, C. Quasi-universal dipolar scattering in cold and ultracold gases. *N. J. Phys.* **11,** 055039 (2009).
26. Gorshkov, A. V. *et al.* Suppression of inelastic collisions between polar molecules with a repulsive shield. *Phys. Rev. Lett.* **101,** 073201 (2008).
27. Wang, D. W., Lukin, M. D. & Demler, E. Quantum fluids of self-assembled chains of polar molecules. *Phys. Rev. Lett.* **97,** 180413 (2006).
28. Klawunn, M., Duhme, J. & Santos, L. Bose-Fermi mixtures of self-assembled filaments of fermionic polar molecules. *Phys. Rev. A* **81,** 013604 (2010).
29. DeMarco, B., Bohn, J. L., Burke, J. P. Jr, Holland, M. H. & Jin, D. S. Measurement of *p*-wave threshold law using evaporatively cooled fermionic atoms. *Phys. Rev. Lett.* **82,** 4208–4211 (1999).
30. Kotochigova, S. Dispersion interactions and reactive collisions of ultracold polar molecules. Preprint at ⟨http://arxiv.org/abs/1003.2672⟩ (2010).

Supplementary Information is linked to the online version of the paper at www.nature.com/nature.

Acknowledgements This work was supported by the US National Institute of Standards and Technology programme Innovations in Measurement Science–Ultracold Stable Molecules, the US National Science Foundation (NSF) Physics Frontier Center at JILA, the US Department of Energy, Air Force Office of Scientific Research Multidisciplinary Research Initiative on Ultracold Molecules, and a NSF graduate fellowship (B.N.).

Author Contributions The experimental work and data analysis were done by K.-K.N., S.O., D.W., B.N., M.H.G.M., J.Y. and D.S.J. Theoretical calculations of the inelastic loss rates were done by G.Q. and J.L.B.

Author Information Reprints and permissions information is available at www.nature.com/reprints. The authors declare no competing financial interests. Correspondence and requests for materials should be addressed to D.S.J. (jin@jilau1.colorado.edu) or J.Y. (ye@jila.colorado.edu).